The 7–13 March 2006 dust storm over West Africa: Generation, transport, and vertical stratification

Pierre Tulet, Marc Mallet, Véronique Pont, Jacques Pelon, A. Boone

The 7–13 March 2006 dust storm over West Africa: Generation, transport, and vertical stratification

Pierre Tulet,[1] Marc Mallet,[2] Véronique Pont,[2] Jacques Pelon,[3] and Aaron Boone[1]

Received 25 January 2008; revised 24 April 2008; accepted 12 May 2008; published 7 August 2008.

[1] Several studies have shown the importance of desert dust aerosols in weather forecast models. Nevertheless, desert dust has been poorly represented in such models and is the source of some prediction errors, in particular for tropical and subtropical regions. The purpose of this paper is to illustrate the formation and the three-dimensional transport of a severe dust storm which occurred in March 2006 over West Africa. An intense dust haze was transported southward over the Gulf of Guinea thereby generating an aerosol optical thickness (AOT) greater than 4 over Nigeria. The MesoNH mesoscale atmospheric model coupled with new dust parameterization schemes has been used to illustrate the three-dimensional transport of the dust plume and the vertical layering of this desert air mass above the lower atmosphere monsoon flux layer. It is modeled that more than 50 g m^{-2} of dust was emitted during this event from the surface by a strong Harmattan wind over the Sahel region. It is also shown that when the dust layer is located over the boundary layer, it can modify the atmospheric stability by as much as 9.5 K in terms of potential temperature in the lowest 2000 m of the atmosphere.

Citation: Tulet, P., M. Mallet, V. Pont, J. Pelon, and A. Boone (2008), The 7–13 March 2006 dust storm over West Africa: Generation, transport, and vertical stratification, *J. Geophys. Res.*, *113*, D00C08, doi:10.1029/2008JD009871.

1. Introduction

[2] Aerosols have long been known to impact the radiative balance of the earth. *Haywood et al.* [1999] found that energy budgets from a global climate model did not match observations from the Earth Radiation Budget Experiment (ERBE) unless aerosols were taken into account. Mineral dust contributes significantly to the global radiative budget through absorption and scattering of longwave and shortwave radiation [*Houghton et al.*, 2001]. At the local scale, high dust concentrations have been shown to impact the vertical structure of the atmosphere thereby modifying convective development [*Lohmann and Diehl*, 2006] and local energy budgets [*Grini et al.*, 2006]. Studies of the effect of dust (and other absorbing aerosols) have been performed using climate models. *Chung et al.* [2002] simulated the climate response to aerosols in a regional climate model over a domain covering the Indian Ocean. They concluded that absorbing aerosols heat the atmosphere and cool the surface which leads to a stabilization of the boundary layer and a reduction in sensible and latent heat fluxes over land. *Chung and Zhang* [2004] have shown that knowledge of the vertical structure of aerosols is crucial in order to determine their impact on the convective available potential energy (CAPE). Recently, a revision of the aerosol climatology in the operational forecast system at European Centre for Medium-Range Weather Forecasts (ECMWF) has led to a significant improvement in the ECMWF 5-day forecasts of the African Easterly Jet, the central dynamical feature over West Africa [*Tompkins et al.*, 2005]. Indeed, it has become a key challenge for weather forecasting models to correctly predict mineral dust transport, concentration and radiative effects in order to improve the representation of atmospheric dynamics and cloud formation in the West African region.

[3] The West African Multidisciplinary Monsoon Analysis (AMMA) field campaign [*Redelsperger et al.*, 2006] provides an excellent opportunity to improve the understanding of the life cycle of desert dust and its feedback with atmospheric dynamics. In particular, the first Special Observing Period (SOP0) of AMMA was devoted to the improvement in the current understanding of the desert dust particle atmospheric processes, especially in terms of their emission and transport from their source areas to their redistribution and sedimentation [*Schepanski et al.*, 2007], and their impacts on the atmospheric radiative budget. During 7–15 March 2006, an intense formation of dust haze was observed over West Africa [*Slingo et al.*, 2006]. This paper is devoted to the analysis of this dust storm, especially in terms of the dust plume formation and its three-dimensional transport. Satellite images derived from MSG-SEVIRI and AQUA-MODIS have been used together with ground observations such as AERONET photometers. The mesoscale MesoNH model [*Lafore et al.*, 1998] coupled with the ORILAM aerosol scheme [*Tulet et al.*, 2005] have been used to explore the capability of the model to represent the

[1] Meteo-France, CNRM, GAME, Toulouse, France.
[2] Laboratoire d'Aérologie, Toulouse, France.
[3] Service d'Aéronomie, Universite Pierre et Marie Curie, Paris, France.

0148-0227/08/2008JD009871

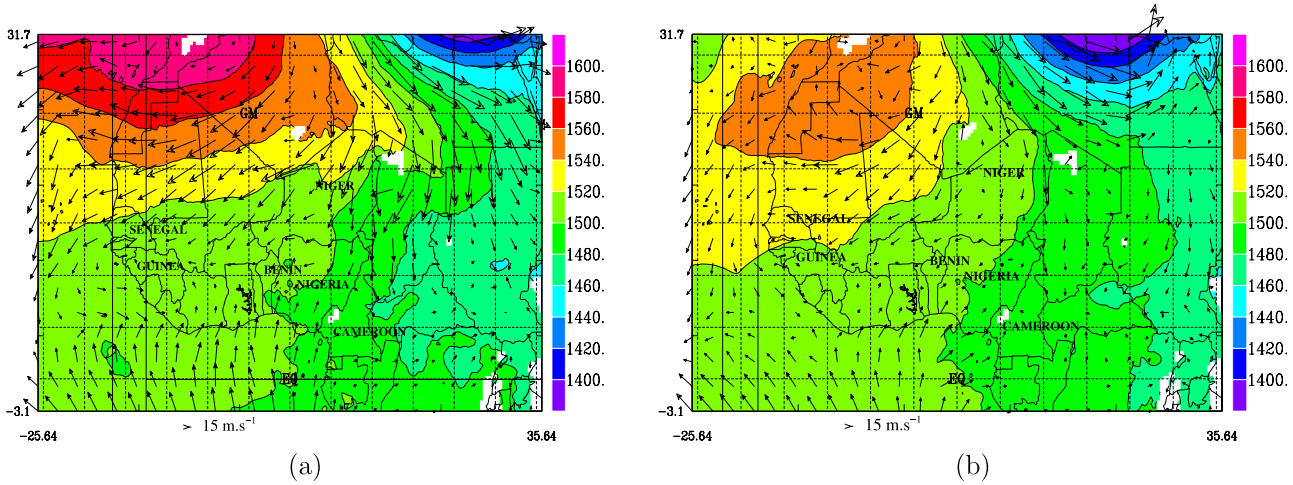

Figure 1. The geopotential at 850 hPa (in meters at the right) and wind field vector (scale of maximum wind vector plotted at 15 m s^{-1}) on (a) 8 March and (b) 12 March 2006.

high levels of dust concentration (section 3). After the validation stage, it is planned to use the model to determine the quantity of dust mass emitted into the atmosphere (section 4) which, in turn, can give an order of magnitude estimation of the soil erosion occurring during West African severe wind storms. The three-dimensional capability of model has been used to show the propagation of dust haze from Niger to the Gulf of Guinea (section 5). Finally, the impact of the dust vertical layering on the atmospheric stability is estimated by comparing the results to a simulation without dust radiative effects. Furthermore, the authors would like to point out that this paper is a complement to studies by *Greed et al.* [2008] and *Milton et al.* [2008] within this issue.

2. The 7–13 March 2006 West Africa Dust Storm

2.1. Synoptic Situation

[4] The 7–13 March 2006 West African dust storm event was characterized by an intense Harmattan wind at the surface which was generated by a strong pressure gradient over West Africa, especially from 7 to 9 March. The 850 hPa geopotential field from 8 March at 1200 UTC from the ECMWF operational analysis (Figure 1a) shows a maximum of 1600 m over Mauritania whereas a deep low was located over Libya which had a minimum height of 1400 m. This strong geopotential gradient lead to an intense surface Harmattan flux over northern Niger (14 m s^{-1}), northern Mali (11 m s^{-1}) and Mauritania (12 m s^{-1}). The Intertropical Discontinuity (ITD), which delineates the dynamic boundary between the Harmattan flux and the monsoon, can be observed at the surface in Figure 1a along a line extending from the northern Ivory Coast to central Nigeria. On 12 March 2006 (Figure 1b), the high-pressure area centered over Mauritania decreased in intensity to 1540 m. As a consequence, the surface wind field decreased over the Sahel region with a maximum value of 8 m s^{-1} located over the northern Mali. The high surface winds over the Sahel during the 7–13 March period lead to a strong dust storm which was readily observed from MSG-SEVIRI satellite images [*Schmetz et al.*, 2002] (Figure 2). *Slingo et al.* [2006] have shown that this dust storm was initiated on 5 March 2006 in the lee of the Atlas Mountains. During the ensuing days, the system propagated southward as a density current moving around the highest topography (e.g., Tibesti). As the flow was channeled through mountains passes, more dust was lifted into the atmosphere. On 8 March, at 1200 UTC (Figure 2a), a dust plume is observed spreading from the desert regions of Mali, Niger and Chad to the southwestern part of the domain. The high dust concentration in the Sahelian African layer contrasts with the cloudy monsoon air mass (in blue) located to the south. Over vegetated regions, the MSG-SEVIRI images cannot retrieve the dust signal which is the reason for the sharp boundary seen between the dusty Sahelian layer and the more southern zone (near the Gulf of Guinea). On 12 March, at 1200 UTC, the dust emission decreased in the desert region (white color in Figure 2b), and the dust particles were transported over the Guinea sea and north of Nigeria.

2.2. AERONET Photometers

[5] During the AMMA program [*Redelsperger et al.*, 2006], five different sites at Djougou (Benin), Ouagadougou (Burkina Faso), M'Bour (Senegal), Banizoumbou (Niger) and Ilorin (Nigeria) were fully equipped with photometric measuring instruments within the framework of the PHOTON network (French part of the Aerosol Robotic Network, AERONET). Such observations can be used to investigate the aerosol optical thickness (AOT) but also, under specific conditions, the aerosol microphysics (volume size distribution) and optical properties (aerosol single scattering albedo, asymmetry factor and refractive index) for the entire atmospheric column [*Dubovik and King*, 2000; *Dubovik et al.*, 2000, 2002]. All of the retrievals of aerosol properties presented in this work were selected at the quality level 2 (cloud-screened data). As shown in Figure 3, the dust activity was very pronounced during the month of March 2006 over a large part of the West African region, especially during the 8 to 15 March period (Figure 3a). The temporal evolution of the AOT (at 440nm), observed over the four PHOTON sites indicates maxima in AOT between 2 and 4, depending on the site. The average AOT (at 440nm) was around 1 during this period for each of the sites, with 1.13, 1.05, 0.99 and 1.24 at Ilorin, Djougou, Banizoumbou and M'Bour, respectively. The time delay of

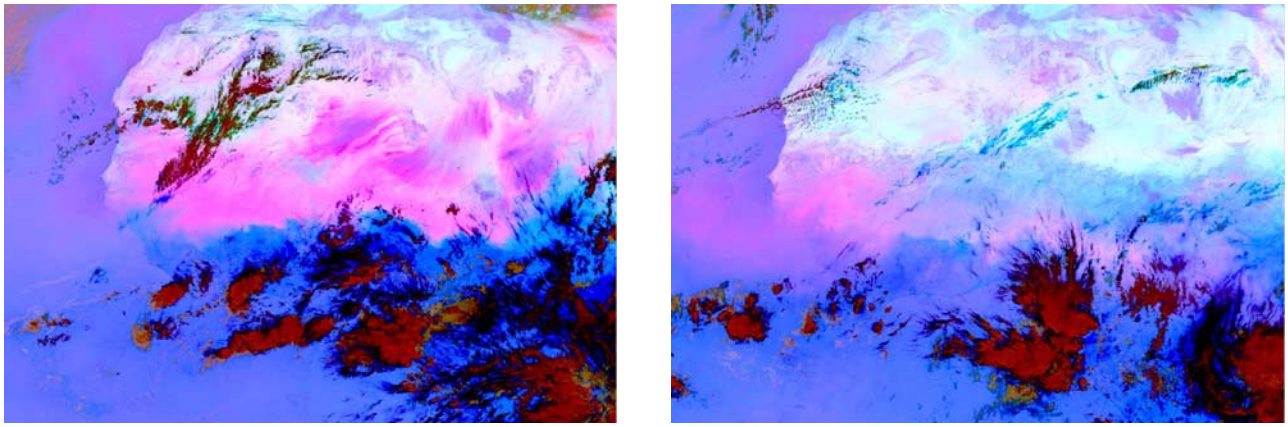

(a) (b)

Figure 2. MSG-SEVIRI satellite images over West Africa for (a) 8 March 2006 at 1200 UTC and (b) 12 March 2006 at 1200 UTC. The images are from the Environmental System Science Centre. Reference colors are computed as a difference of wavelengths using an EUMETSAT algorithm: the pink color represents dust, black is for cirrus, red is for high-level cloud, brown is for the midlevel cloud, and white is for the desert surface.

the AOT increases during the period 7 to 12 March, between the Banizoumbou and the Ilorin sites clearly reveals the propagation of the dust storm in the southern part of the study domain. Therefore the increases of AOT at M'Bour also show a dust plume reaching Senegal (western part of the domain). The spatial extents of both plumes are consistent with MSG/SEVERI satellite observations (Figure 2).

[6] The uncertainty in AOT measurements is about ±0.01 [*Holben et al.*, 2001]. Figure 1b also shows the temporal evolution of the Angstrom exponent, which was calculated from the wavelength pair 440 and 870 nm. It shows a significant decrease of $\alpha_{440/870}$ during the dust event with very low values (around 0.2), indicating the presence of very large particles over the West African region during the period.

3. Simulation Evaluation

3.1. MesoNH Model

[7] The mesoscale-scale, nonhydrostatic atmospheric model MesoNH was used in this study. This model has been jointly developed by the Centre National de la Recherche Meteorologique (CNRM, Meteo France) and the Laboratoire d'Aérologie (LA, CNRS) [*Lafore et al.*, 1998]. MesoNH can be used to simulate small scale (Large Eddy Simulation type) to synoptic scale phenomena (horizontal resolution ranging from a few meters to several tens of kilometers), and it can be run in a two-way nested mode involving up to 8 nests. Parameterizations are included for convection [*Bechtold et al.*, 2001], cloud microphysics [*Cohard and Pinty*, 2000], turbulence [*Bougeault and Lacarrére*, 1989], biosphere-atmosphere exchanges [*Noilhan and Mahfouf*, 1996], urban-atmosphere interactions [*Masson*, 2000], lightning processes [*Barthe et al.*, 2005], gaseous chemistry [*Suhre et al.*, 1998; *Tulet et al.*, 2003] and chemical aerosols [*Tulet et al.*, 2005].

[8] The dust aerosol processes are parameterized following *Grini et al.* [2006]. This parameterization uses the three dust aerosol modes of *Alfaro and Gomes* [2001], which evolve using the ORILAM lognormal aerosol scheme [*Tulet et al.*, 2005]. Vegetation types are prescribed from the ECOCLIMAP database [*Masson et al.*, 2003], where two surface classes have been used to identify dust source areas: "no vegetation with rocks" and "bare soil." This study has therefore assumed that the lack of vegetation for a particular land cover type corresponds to a potential dust source zone. The soil texture information includes the percentage of clay and sand, and these data are from the Food and Agriculture Organization database [*Food and Agriculture Organization*, 1988]. For emission processes, dust is mobilized using the Dust Entrainment And Deposition model (DEAD) [*Zender et al.*, 2003]. DEAD calculates fluxes of dust from the surface layer friction velocity, the soil wetness index and the percentage of clay and sand in the soil. The physical basis of the model is taken from *Marticorena and Bergametti* [1995], for which dust is parameterized as a function of saltation and sandblasting. The dust emissions are forced directly by the surface flux parameters of the land surface scheme, and then distributed into the atmosphere in a manner which is consistent with the vertical fluxes of momentum, energy and moisture.

[9] MesoNH uses the ECMWF radiative transfer model [*Fouquart and Bonnel*, 1980; *Morcrette and Fouquart*, 1986; *European Centre for Medium-Range Weather Forecasts* (*ECMWF*), 2004]. Clouds and aerosols in the shortwave spectral region are taken into account using the delta Eddington transformation [*Joseph et al.*, 1976]. For shortwave effects, a refractive index of the dust aerosols is obtained using AERONET [*Dubovik and King*, 2000; *Dubovik et al.*, 2000] retrievals for each site. The values of the refractive indexes used in the radiative transfer computations are

[10] $-R_i = 1.448\text{-}0.00292i$ for wavelengths between 0.185 and 0.69μm.

[11] $-R_i = 1.44023\text{-}0.00116i$ for wavelengths between 0.69 and 1.19μm.

[12] $-R_i = 1.41163\text{-}0.00106i$ for wavelengths between 1.19 and 4.0 μm.where i represents the complex index of the Refractive Index (R_i). The standard formulation of

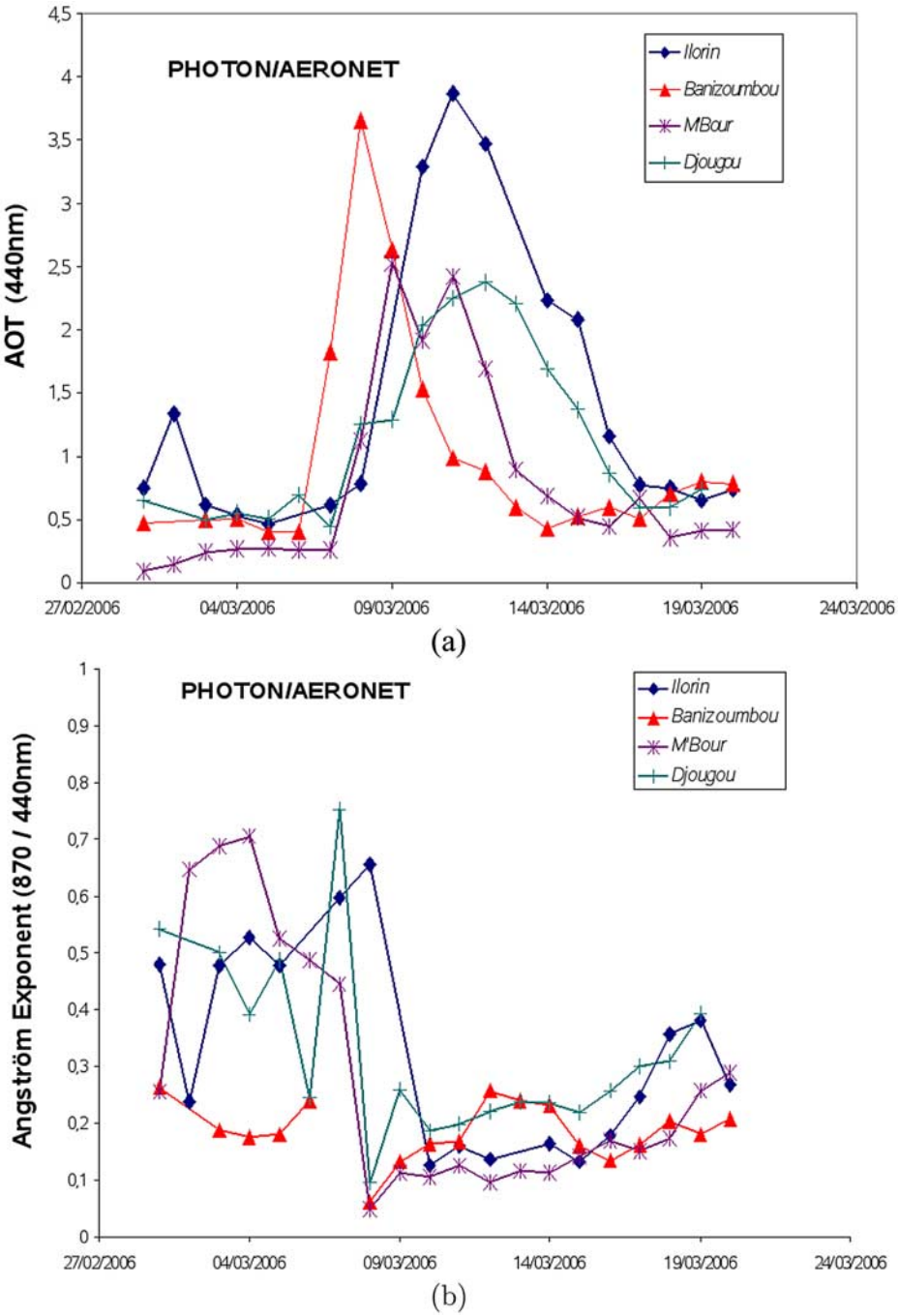

Figure 3. (a) The aerosol optical thickness at 440 nm and (b) the Angstrom coefficient trends between 1 March 2006 and 22 March 2006.

absorption and reemission of longwave radiation for aerosols from the ECMWF model is used. In this formulation, a fraction of the 550 nm aerosol optical depth is added to the longwave optical depth for CO_2 and H_2O, which in turn is used to calculate absorption and reemission of longwave radiation. The fraction is constant for each longwave band and aerosol type [*ECMWF*, 2004].

3.2. Simulation Configuration

[13] The simulations started at 0000 UTC on 6 March 2006 and ended at 0000 UTC on 14 March 2006. The first day of the simulation has been used as a model spin-up period. A two-way nested grid domain was used: the large domain (36-km resolution) is defined between 3.1°S and 31.7°N latitude and 25.64°W and 35.64°E longitude. This area represents the so-called "large West Africa region" where most of the potential dust sources have been included. The smallest embedded domain (12-km resolution) is centered over northwestern Nigeria and it covers a large part of the AMMA field campaign domain (4.3°N and 17.6°N latitude and 4.19°W and 16.24°E longitude). The vertical resolution consisted in 60 stretched vertical levels reaching an altitude of 34000 m, and half of the levels were located in the boundary layer between the surface and

2000 m. Initial and lateral boundary conditions for the large domain were taken from the ECMWF operational analysis. For dust, both the initial and the boundary concentrations have been set close to zero. Indeed, background dust is not included in the model and all of the atmospheric particulate matter are generated within the domain of simulation. The initial soil wetness index (SWI) was computed in offline mode (decoupled from the atmospheric model) using low-level atmospheric data from the ECMWF forecast model merged with satellite precipitation data from the EPSAT-SG product [*Chopin et al.*, 2004] and downwelling shortwave and longwave atmospheric radiative fluxes from the LAND-SAF product [*Geiger et al.*, 2008]. These forcing data were then used as an upper boundary condition to drive the ISBA land surface model from 2004 to 2006 in order to obtain a soil moisture state which is more realistic than that obtained from operational NWP models. See *Boone and deRosnay* [2007] for further details on the forcing data and the methodology.

3.3. AOT During 7 to 13 March 2006

[14] The evolution of the Sahelian dust AOT simulated by MesoNH in the large domain is shown in Figures 4a–4c. After 2 days of model integration, a strong belt of high AOT develops in an area from Chad to Senegal (Figure 4a). Several different AOT maxima have been simulated in central Libya (3.2), Chad (3.4), the Darfour area (2.6), the southern Niger and the northern Nigeria (3.2). This high AOT band is consistent with MSG-SEVIRI images (Figure 2a). On 10 March (Figure 4b), the dust plume (region of high AOT) spread to the south to the Gulf of Guinea. In particular, three intense AOT maxima (with values exceeding 3.2) have been simulated around Nigeria (from Benin to southern Chad and Cameroon). On 12 March the intense dust plume was still present to the south over the Guinea Sea and the Atlantic Ocean. The AOT decreased overall within the domain, but there were still significant peaks exceeding 1.6 from Nigeria to Ghana, and reaching values of 2 and 2.6 over Guinea and the Gulf of Guinea, respectively.

[15] The evolution of the AOT can be seen in the observational data from AQUA-MODIS satellite (Figures 4d–4f). The areas where data are missing correspond to either cloudy regions or locations over the desert were the soil albedo is too large. These data were obtained from MODIS data collection 5 using the MODIS online visualization and Analysis System (MOVAS) developed at NASA (http://daac.gsfc.nasa.gov/techlab/giovanni/G3_manual_Chapter_8_MOVAS.shtml). It is interesting to note that there was fairly good agreement between the MesoNH simulation and the satellite observations during the event. In particular, on 8 March (Figures 4a and 4d), the dust plume did not reach the Gulf of Guinea and was located over northern Benin and central Nigeria. With the exception of southeast Nigeria and northern Cameroon, the location of high AOT compares well in terms of location and intensity between MODIS and MesoNH. Note that the AOT simulated by MesoNH corresponds to dust aerosols only, otherwise all aerosols types have been integrated by MODIS in the computation of AOT. On 10 March it is interesting to note that the AQUA-MODIS satellite also retrieved three AOT maxima exceeding 3 in the same location around Nigeria (Figure 4e). Moreover, the dust plume observed over Guinea and the Atlantic Ocean was reproduced in the simulation. Only the high AOT of 3 simulated over Sudan is not observed by the MODIS instrument. On 12 March the AQUA-MODIS observed some high values of AOT over Benin, Nigeria and Cameroon exceeding 3 in the coastal areas. These AOT values are higher than those simulated, showing a probable drift of the model after 6 days of forecast integration.

[16] During the AMMA campaign, AERONET photometers were located at Ouagadougou (Burkina Faso), Ilorin (Nigeria), Djougou (Benin) and Banizoumbou (Niger). The observed AOT has been compared to the simulation (Figure 5). As shown before, the four aforementioned stations have high levels of AOT from 7 to 13 March 2006. The Banizoumbou station (Figure 5a) is located in the Sahelian area of Niger where the observed strong winds generated a significant dust emission. AOT values exceeding 3 have been observed on 7 March, and they reached values up to 4.0 on 8 March. At Banizoumbou, which is the AERONET station closest to the dust source zone, the simulated AOT compared well with that observed. In particular, the peaks observed on 8 and 9 March were well reproduced for the AOT, which decreased after 10 March. In addition, the model clearly reveals two nighttime peaks of AOT between 8 and 10 March. This diurnal variation can be attributed to the near surface nocturnal jet [*Parker et al.*, 2005; *Lothon et al.*, 2008]. The emission was particularly intense in this area because of the soil composition of mainly sand: heat is stored in a thin soil layer resulting in a more significant radiative surface cooling during night which reinforces the nocturnal stable stratification. This stratification results in an intense of the nocturnal jet and a maximum of dust mobilization during the night (as is also reported by *Chaboureau et al.* [2007]). The AOT simulated over Ouagadougou is well reproduced except for 10 March. The AOT over Djougou is accurate from 9 to 10 March, but it is underestimated for the other days of the simulation. The AOT over the Ilorin station in southern Nigeria is significantly underestimated; the maximum simulated AOT reached 2.6, whereas the photometers registered AOTs above 4. At this stage, the authors do not have sufficient evidence to determine whether the origin of this underestimation is attributable to an underestimation of the simulated dust emission over Niger (surface winds) or to the more local carbonaceous aerosols. Nevertheless, at Ilorin, the model was able to reproduce the delay in the increase of the AOT observed after 9 March. Thus a systematic underestimation of AOT (about 1) also appeared at Djougou when the station was in the monsoon flux. This bias can be attributable to carbonaceous aerosols (black and organic carbon fractions) which are not included in the simulation. Indeed, for Angstrom coefficients given by photometer measurements at Djougou over the simulated period, the mean value reached 0.22 ± 0.03. This low value implies a high contribution of large particles in the atmospheric column. Nevertheless, as shown in Figure 6, lower atmospheric layers were loaded with combustion aerosols due to black carbon concentrations (measured with an aethalometer at surface). These particles could be of various origins and are presumably from anthropogenic sources and biomass burning. The MODIS response rapid active fire (http://maps.geog.umd.edu/products/animation/2006_animation.gif) product shows that biomass burning was widespread

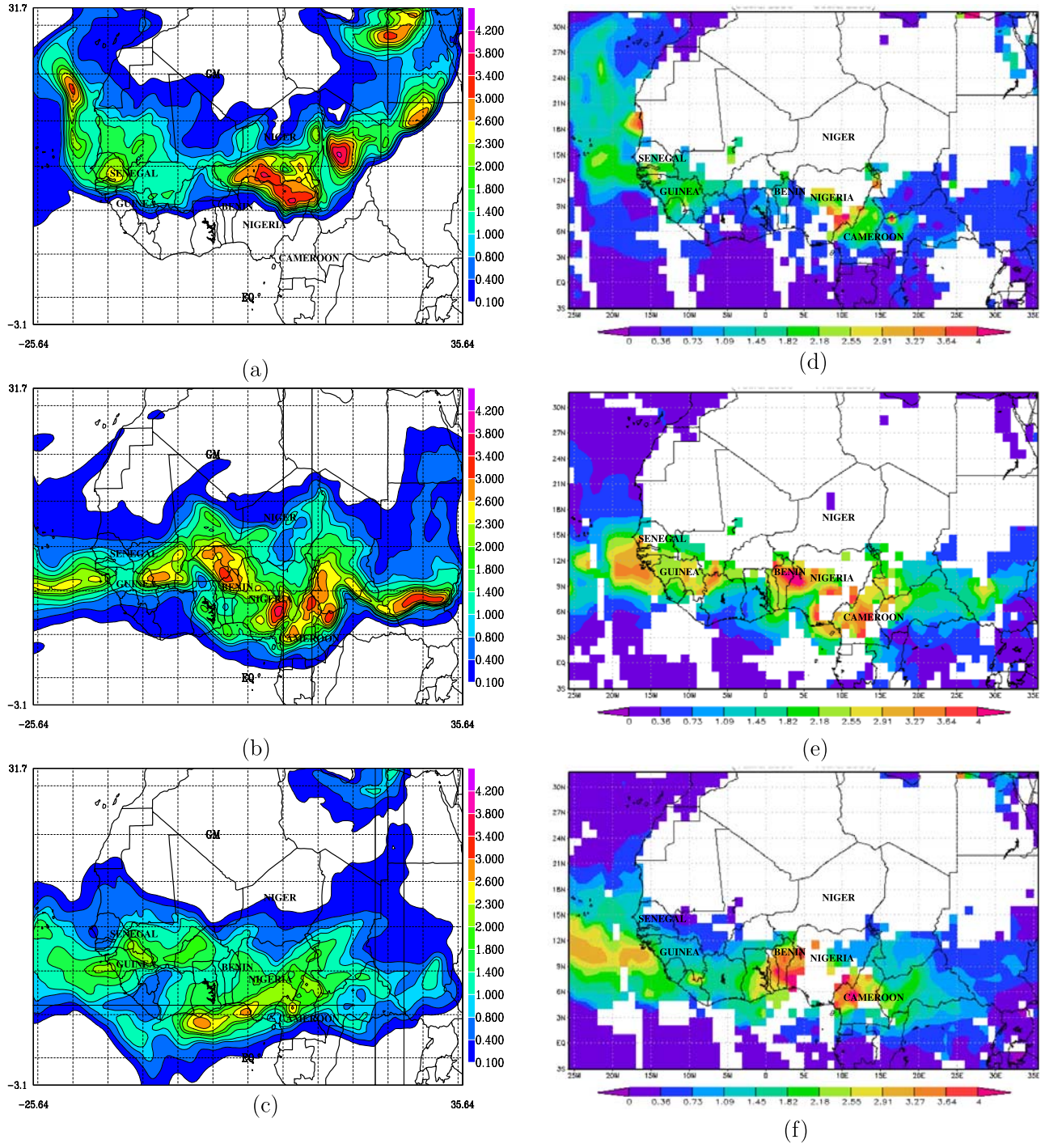

Figure 4. AOT restricted to dust, simulated by MesoNH (36 km of resolution) on (a) 8 March at 1200 UTC, (b) 10 March at 1200 UTC and (c) 12 March at 1200 UTC 2006. The daily mean AOT from MODIS/AQUA satellite images on (d) 8 March, (e) 10 March, and (f) 12 March 2006.

during March 2006. Moreover, in Figure 6, the dotted and crossed lines show the mean concentration of black carbon observed, respectively, in May 2006 (no fires during this month) and January 2006 (a high fire occurrence) at Djougou. For both of these months, the AERONET 440 nm AOT and Angstrom coefficient were consistent with these ground observations: high AOT (between 0.9 and 1.4) and Angstrom coefficients (between 0.8 and 1.2) in January 2006, and low AOT (around 0.5) and Angstrom coefficient (around 0.3) in May 2006. During March 2006, high black carbon concentrations were observed over Benin (monthly mean value of 2300 ± 700 ng m^{-3}). Moreover, note that from 9 to 12 March, black carbon concentrations were higher than the monthly mean value, showing a significant load of combustion aerosols in the lower atmosphere. Therefore, not only active fire aerosols emissions but also background combustion aerosols concentrations could explain the underestimation of the simulated AOT, as these highly optically interactive

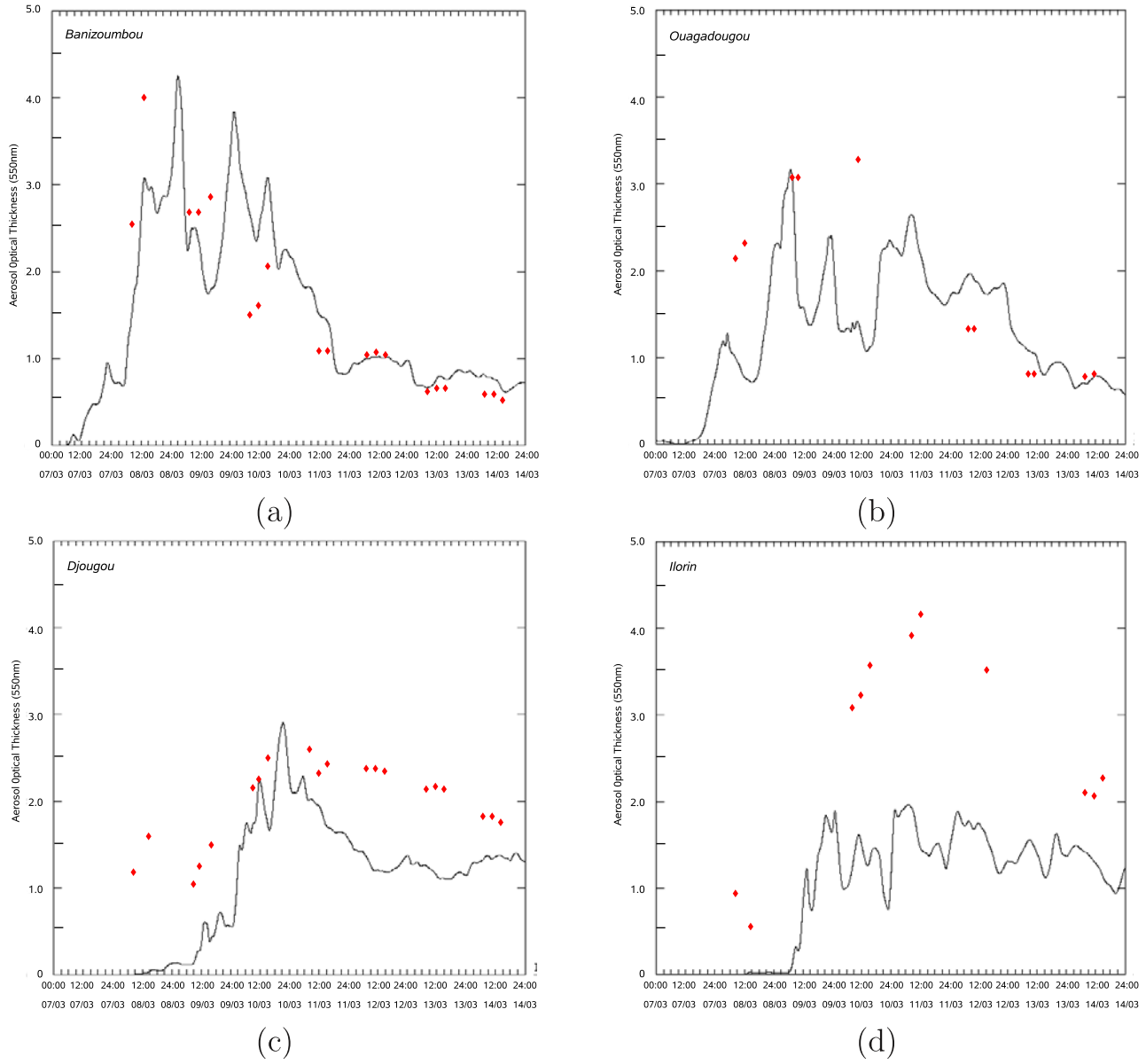

Figure 5. The evolution of the AOT simulated by MesoNH between 7 and 13 March 2006 at (a) Banizoumbou, (b) Ouagadougou, (c) Djougou, and (d) Ilorin. The dots represent the photometer observed values.

carbonaceous aerosols were not taken into account in our MesoNH simulations. In the following sections, a higher resolution simulation (using grid nesting) illustrates that these sites were located within a strong AOT gradient which could explain differences between the observations and the simulation.

4. Modeled Dust Generation

[17] It was shown that the model correctly estimated the order of magnitude of the AOT which were observed during the storm of 7–13 March. The next step is to estimate the desert dust flux emitted during this period. The emitted dust maximum occurred on 8 March, around 0000 UTC (Figure 7a). At this time, the modeled surface wind exceeded 13 m s^{-1} over Niger and northern Chad. The intense wind over these regions generated sandblasting and saltation [*Marticorena and Bergametti*, 1995] between sand and clay aggregates that produced a modeled dust mass flux of more than 300 μg m^{-2} s^{-1} which was emitted to the atmosphere. In other areas, such as Mali and Mauritania where the wind speed was still significant but less than 10 m s^{-1}, the dust mass flux was approximately 20 to 80 μg m^{-2} s^{-1}. All of these regions are semiarid and therefore correspond to soil surfaces without vegetation and with low SWI in the model: these factors play an important role in the amount of the simulated dust flux (in addition to the wind speed intensity). Note that these sources of simulated dust emission correspond to the Saharan dust source activation frequency map derived from MSG-SEVIRI of *Schepanski*

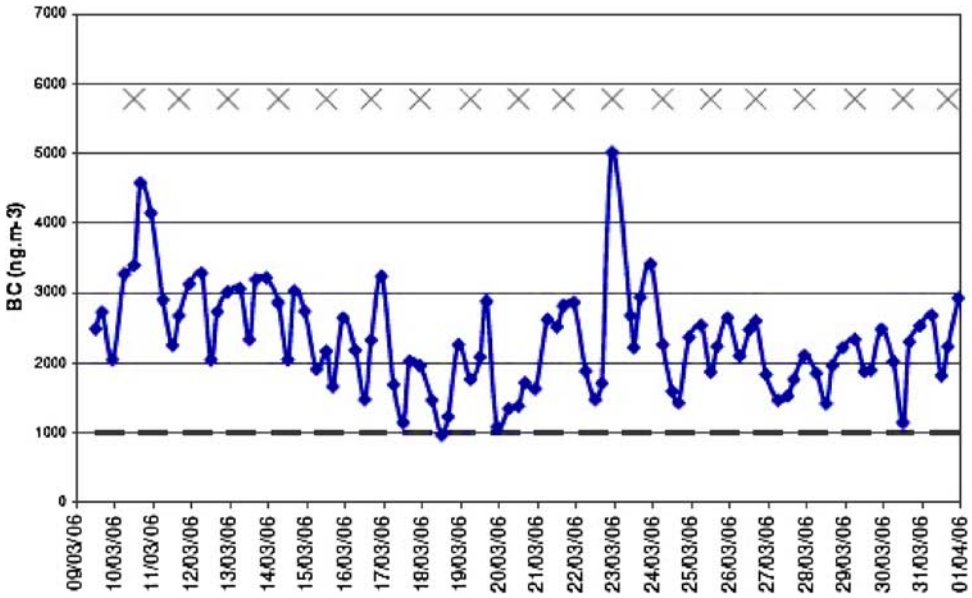

Figure 6. Black carbon surface concentrations from 9 March 2006 to 31 March 2006 at Djougou. The dotted line stands for the May mean concentration (beginning of the wet season), and the line of crosses stands for the January mean concentration (month of intense biomass burning emissions).

et al. [2007]. The integration of the dust mass flux during the four most intense days of the period from 7 to 11 March (inclusive), gives an order of magnitude estimate of the total wind erosion. As shown in Figure 7b, this erosion reached a maximum value of 60 g m^{-2} over Niger. The entire Sahelian belt emitted a significant mass of dust greater than 1 g m^{-2}, showing that this region was characterized by a strong surface wind during the period. In addition to Niger, two other significant dust source zones have been identified (see Figure 7b): over Libya with a maximum of 30 g m^{-2}, and over Mauritania with a maximum of 20 g m^{-2}. These high values show the importance of wind erosion during such an event. In addition, this analysis shows how the soil composition can rapidly evolve in such semiarid African regions during intense wind episodes. Indeed, wind erosion is a selective process that implies the removal of the finest soil particles that contain the greatest amount of nutrients and leaves the coarsest soil particles (like sand) at the surface near the source areas [*Nickling and Gillies*, 1989; *Shao et al.*, 1993].

5. Dust Transport and Vertical Stratification

5.1. AOT Evolution in the AMMA Area

[18] The dust spatial distribution during the period 8–11 March is analyzed in more detail in this section. Figure 8 shows the AOT simulated at the 12 km resolution over Niger, Nigeria, Burkina Fasso and Gana. On 8 March the dust plume was still located in the northern part of the domain. High AOT values greater than 3 were simulated over Niger which were associated with strong surface winds reaching 13 m s^{-1}. Over Nigeria, the AOT was still low

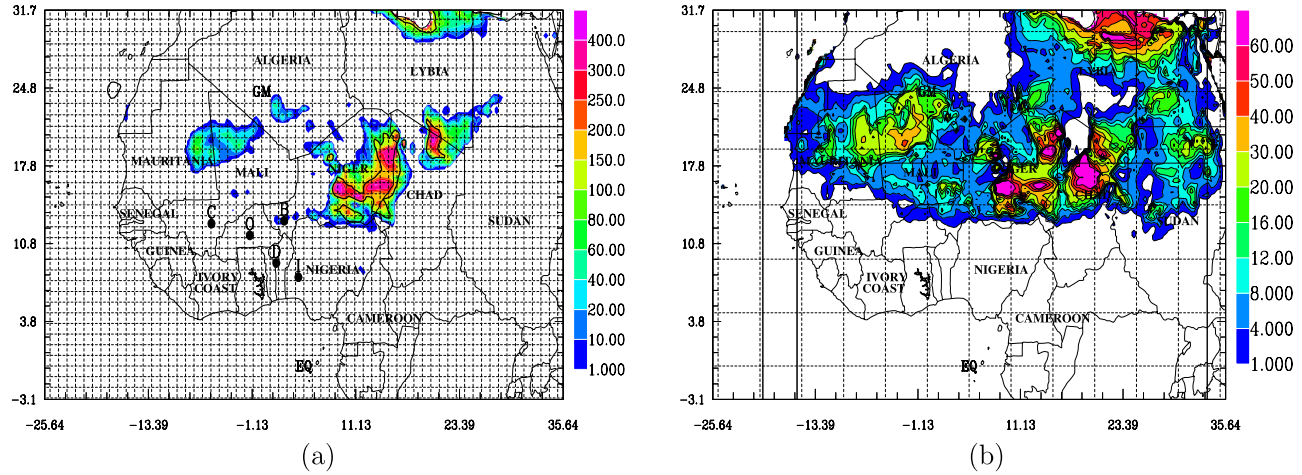

Figure 7. (a) The dust mass flux emitted on 8 March at 0000 UTC (μg m^{-2} s^{-1}) and (b) the dust mass integrated flux between 7 March at 0000 UTC and 11 March at 0000 UTC (g m^{-2}). The isocontour indicates the zone where the surface wind is greater than 10 m s^{-1}.

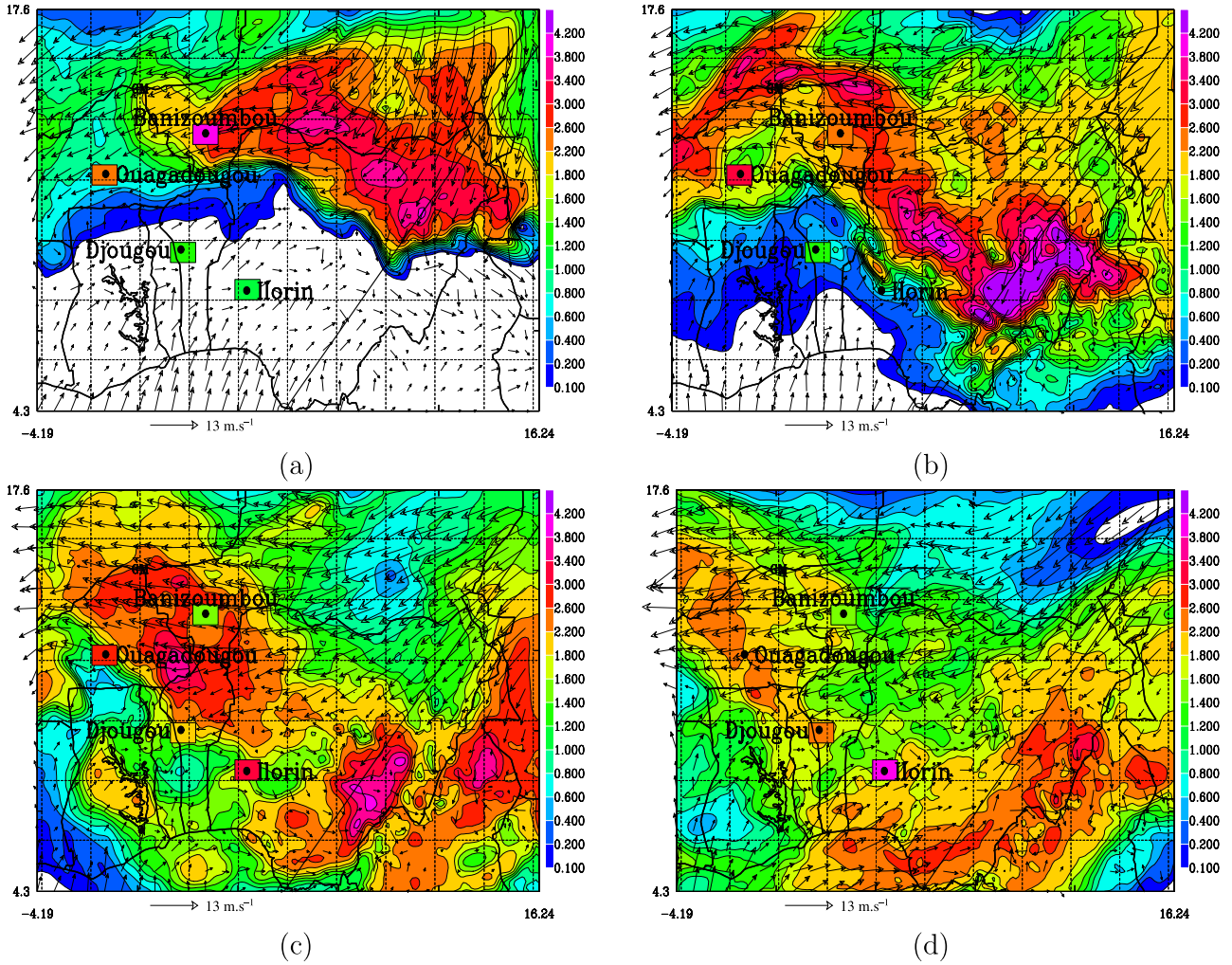

Figure 8. AOT simulated by MesoNH (12 km of resolution) on (a) 8 March at 1200 UTC, (b) 9 March at 1200 UTC, (c) 10 March at 1200 UTC, and (d) 11 March at 1200 UTC. The surface wind field has been superimposed (scale of maximum vector plotted is equal to 13 m s^{-1}). The plain line represents the vertical cross section of Figure 9. The squares indicate the AOT/AERONET observed values.

(and similar to those observed over Ilorin). In comparison to photometer observations (colored squares), the model underestimates the AOT (of 1) at Djougou and Ilorin during the first days of the simulation. Prior to 9 March these two stations were located within the monsoon flux (not shown). Because there is no dust source south of Djougou and Ilorin, this underestimation could not be attributable to a lack of dust initialization in the model. Indeed, as mentioned in section 3.3, it is assumed that this underestimation can be due to nondesert aerosols which are often present in the monsoon layer and not taken into account by the model. Nevertheless, the gradient associated with large AOT in the north (Banizoumbou), moderate AOT in the central part of the domain (Ouagadougou) and small AOT in the south (Djougou and Ilorin) have been well simulated. The Intertropical Discontinuity (ITD) can be observed at the surface in terms of the convergence of southwesterly winds (monsoon flux) and northeasterly winds (Harmattan flux) observed from the north of Nigeria to the north of Ghana. On 9 March the northeasterly winds slightly decreased to 10 m s^{-1}, but the frontal zone appeared further south in the central part of Nigeria. The simulated and observed dust increases correspond to very high AOT values with a maximum of 5 over Nigeria (Figure 8b). The AOT decreased on 10 March, but it remained significant with three distinct maxima of 3.4 over Nigeria (Figure 8c). In comparison with the photometric observations (colored squares) at Banizoumbou and Ouagadougou, note that the dust plume is probably simulated too far east. This can be attributed to an underestimation of the easterly winds simulated in this area. On 11 March the Harmattan flux decreased to 8 m s^{-1}, and correspondingly the monsoon wind increased to 5 m s^{-1} (Figure 8d): the location of the surface ITD moved to the north. On this day, it is interesting to note that a large value of AOT was located along the Gulf of Guinea where the wind regime is mainly southwesterly. This feature can be explained by a transport of dust located above the monsoon flux: this is described in more detail in the next section.

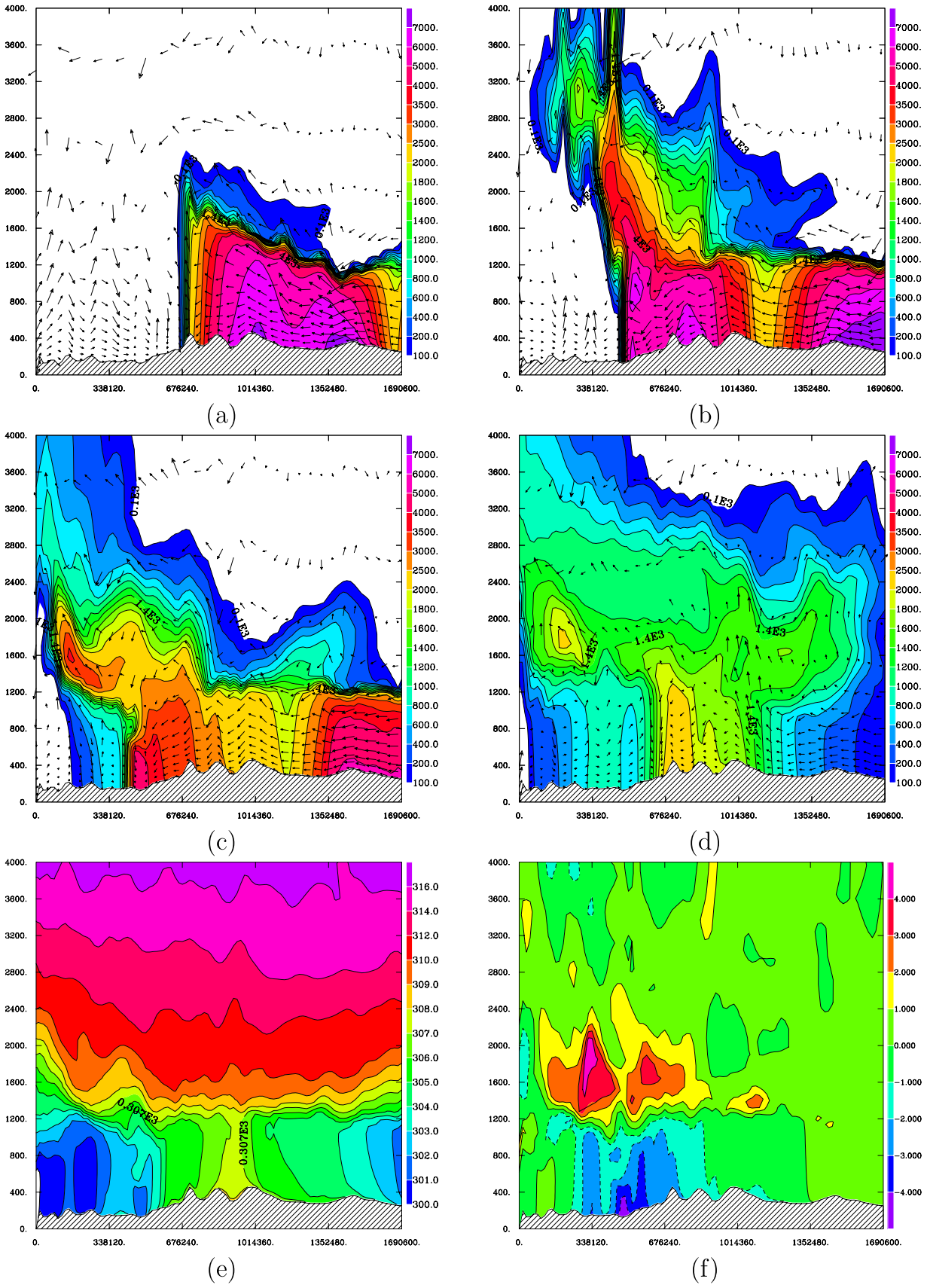
(a)
(b)
(c)
(d)
(e)
(f)
0.1E3
1.4E3
0.307E3
0. 338120. 676240. 1014360. 1352480. 1690600.

Figure 9

5.2. Dust Vertical Stratification

[19] In order to better understand this vertical layering of the atmospheric dust, a vertical cross section was made along the plain line in Figure 8. This cross section (Figure 9) shows the total dust mass of the 3 modes between the surface and 4000 m. On 8 March (Figure 9a), the main dust concentration was still located mostly in the Sahelian area in northern of Nigeria. In this source zone, large wind speeds (in excess of 13 m s^{-1}) produced a very high concentration of dust which reached a maximum value of 6000 μg m^{-3} near the surface. The aerosols were well mixed in the Sahelian boundary layer up to an altitude of approximately 1200 m above the surface. The convergence of Harmattan and monsoon surface winds along the ITD frontal zone lift the aerosols upward to 2000 m. On 8 March the ITD is delineated by the strong gradient of mineral dust observed in the middle of the cross section of Figure 9a. This phenomenon increased on 9 March (Figure 9c), with a significant transport of dust above the surface monsoon layer. More than 2000 μg m^{-3} of dust reached an altitude of 3000 m. On 10 March, as the dust production decreased in the Sahelian source region, an intense dust layer with a maximum concentration of 3500 μg m^{-3} was simulated above the monsoon flux over the central part of Nigeria. This dust layer, which was located above the monsoon flux, increased on 11 March, to a thickness of 3000 m (Figure 9d). This high dust concentration layer reached all the way to the Gulf of Guinea (as was shown in section 5.1). The sedimentation of coarse aerosols corresponds to the presence of dust (about 500–1000 μg m^{-3}) in the monsoon layer on 10 and 11 March.

[20] The impact of this dust layer on the atmospheric dynamics is evaluated using MesoNH by comparing the simulation with (DUST) and without (NODUST) dust. A detailed study of this topic has been made by M. Mallet et al. (A study of the impact of Saharan dust on the radiative forcing, surface energy budget and atmospheric dynamics over the West African region in March 2006, manuscript in preparation, 2008), whereas the current study focuses on the dynamical impact on the modification of the vertical potential temperature profile due to the presence of the dust layer. Figure 9e shows the vertical structure of the potential temperature on 10 March. The monsoon layer is slightly colder than the Harmattan layer, and both the monsoon and the Sahelian boundary layers are characterized by a well mixed potential temperature between the surface and a height of 1000 m. The ITD is characterized by isentropes which are curved above the monsoon flux. This zone is stable and separates the monsoon layer from the overlying dust layer. The difference in potential temperature between the DUST simulation and the NODUST simulation is shown in Figure 9f. It can be seen that the absorption of solar radiation by dust particles heats the dust layer with a maximum difference of 5 K. As a consequence, the solar radiation reaching the surface is lower and the air temperature under the dust layer has been decreased by 4.5 K. This shows that dust increased the stable stratification between the monsoon layer and the overlying Harmattan layer located in the ITD area. This stratification increased the stability of the lower atmosphere by approximately 9.5 K in the 2000 m above the surface. This change in the potential temperature profile represents a significant modification of the Convective Available Potential Energy (CAPE) which, in turn, could change the initiation of convection or more generally the cloud formation over the area affected by this Sahelian dust layer.

6. Conclusion

[21] This study was devoted to the description and analysis of simulation of the 7–13 March dust storm which occurred during the SOP0 of the AMMA campaign. The SEVIRI-MSG images revealed high-altitude plumes of desert dust which were generated over the West African Sahelian region and then transported southward and westward in the direction of the Gulf of Guinea and the Atlantic ocean. This was observed by the AERONET photometers located over West Africa, where AOT exceeded 2 after 8 March, and then reached values of 3.5 and 4.0 over Niger and Nigeria, respectively. The decrease of the Angstrom coefficient during the event revealed the presence of very large suspended particles.

[22] The coupled modeling of dust particles using the mesoscale model MesoNH was a very useful tool in order to improve the understanding of such dust storm events, from the formation of atmospheric dust in the Sahelian region, to its vertical and horizontal transport, and finally to its feedbacks with the atmospheric dynamics. The MesoNH simulated AOT were in good agreement with the local Photometer observations over Niger and Nigeria. In particular, the model accurately reproduced the time delay of the propagation of the dust from Niger and Chad to Nigeria and the Gulf of Guinea. The simulated AOT and that retrieved from the MODIS images on the AQUA platform were of the same order of magnitude and the maxima were located in similar locations. This shows that the recent joint evolution of models and satellites could give some useful information on the spatial representation of aerosols. This is particularly significant for a large part of the West African region where local observations are relatively sparse.

[23] Furthermore, the simulation was used to determine the source regions where the model generated the saltation of dust particles, and it gave reasonable estimates of the order of magnitude of the total mass emitted into the atmosphere. In some areas, the total mass flux modeled exceeded 50 g m^{-2} during the four most windy days of the studied period. This shows the importance of soil erosion which is significant during this event, and it illustrates the rapid possible change in the near-surface soil composition of some African semiarid regions and surrounding areas.

Figure 9. The vertical cross section of dust mass (μg m^{-3}) simulated by MesoNH on (a) 8 March at 1200 UTC, (b) 9 March at 1200 UTC, (c) 10 March at 1200 UTC, and (d) 11 March at 1200 UTC. (e) The vertical cross section of potential temperature (K) simulated by MesoNH on 10 March at 1200 UTC and (f) difference in potential temperature (K) between DUST and NODUST simulations on 10 March at 1200 UTC. The horizontal line is for the vertical cross section from Figure 8.

[24] Finally, the 3-D structure of the dust plume propagation was detailed using a nested domain at a 12km resolution in order to represent the layering of the dust above the monsoon flux in more detail. The model showed the high spatial variability of the dust AOT over Nigeria which comprises values ranging between 1 and 4. This reveals the limit of local predictability of fields in areas associated with strong gradients. The determination of the position of the ITD is quite difficult, and the location evolved rapidly during the study period over Niger and Nigeria. The dust plume generated within the Harmattan flux was lifted above the monsoon flux, thereby increasing the vertical stable stratification by absorbing a significant fraction of the incoming solar radiation. This modification of the lower atmospheric stability reached about 9.5 K within the lowest 2000 m of the atmosphere. This type of stratification can generate some large modifications of the atmospheric dynamics and cloud formation. A detailed study of these modifications is presented by Mallet et al. (manuscript in preparation, 2008). More generally, this increased stable stratification resulting from the presence of dust in the Saharan layer could have a significant impact on the cyclogenesis of the Atlantic tropical cyclones [*Dunion and Velden*, 2004].

[25] **Acknowledgments.** On the basis of a French initiative, AMMA was built by an international scientific group and is currently funded by a large number of agencies, especially from France, UK, US, and Africa. It has been the beneficiary of a major financial contribution from the European Community's Sixth Framework Research Program. Detailed information on scientific coordination and funding is available on the AMMA international Web site (http://www.amma-international.org). We particularly thank P. Goloub, L. Blarel, T. Podvin, and their staff for establishing and maintaining the Djougou, Banizoumbou, Ilorin, and M'Bour sites used in this investigation. We also would like to thank the MesoNH assistance team for their support and availability. Finally, we also want to thank Gary Robinson of the Environmental Systems Science Centre for providing free access to their MSG-SEVIRI images used in this study. The Web site managed by ESSC is a real help offered to the AMMA community to interpret IOP. The authors also thank A. Mariscal for the aethalometer measurements in Djougou.

References

Alfaro, S. C., and L. Gomes (2001), Modeling mineral aerosol production by wind erosion: Emission intensities and aerosol size distributions in source areas, *J. Geophys. Res.*, *106*(D16), 18,075–18,084.

Barthe, C., G. Molinié, and J. Pinty (2005), Description and first results of an explicit electrical scheme in a 3D cloud resolving model, *Atmos. Res.*, *76*(1–4), 95–113.

Bechtold, P., E. Bazile, F. Guichard, P. Mascart, and E. Richard (2001), A mass-flux convection scheme for regional and global models, *Q. J. R. Meteorol. Soc.*, *127*, 869–886.

Boone, A., and P. deRosnay (2007), AMMA forcing data for a better understanding of the West African monsoon surface-atmosphere interactions, in *Quantification and Reduction of Predictive Uncertainty for Sustainable Water Resource Management*, *IAHS Publ.*, *313*, 231–241.

Bougeault, P., and P. Lacarrére (1989), Parametrization of orography-induced turbulence in a meso-beta model, *Mon. Weather Rev.*, *117*, 1872–1890.

Chaboureau, J.-P., P. Tulet, and C. Mari (2007), Diurnal cycle of dust and cirrus over West Africa as seen from Meteosat Second Generation satellite and a regional forecast model, *Geophys. Res. Lett.*, *34*, L02822, doi:10.1029/2006GL027771.

Chopin, F., J. Berges, M. Desbois, I. Jobard, and T. Lebel (2004), Multiscale precipitation retrieval and validation in african monsoon systems, paper presented at 2nd International TRMM Science Conference, Jpn. Aerospace Explor. Agency, Nara, Japan, 6–10 Sept.

Chung, C., and G. Zhang (2004), Impact of absorbing aerosol on precipitation: Dynamic aspects in association with convective available potenaitl energy and convective parameterization closure and dependence on aerosol heating profile, *J. Geophys. Res.*, *109*, D22103, doi:10.1029/2004JD004726.

Chung, C., V. Ramanathan, and J. Kiehl (2002), Effects of the south Asian absorbing haze on the northeast monsoon and surface-air heat exchange, *J. Clim.*, *15*, 2462–2476.

Cohard, J., and J. Pinty (2000), A comprehensive two-moment warm microphysical bulk scheme. II: 2D experiments with a non hydrostatic model, *Q. J. R. Meteorol. Soc.*, *126*, 1843–1859.

Dubovik, O., and M. D. King (2000), A flexible inversion algorithm for retrieval of aerosol optical properties from Sun and sky radiance measurements, *J. Geophys. Res.*, *105*, 20,673–20,696.

Dubovik, O., A. Smirnov, B. Holben, M. King, Y. Kaufman, T. Eck, and I. Slutsker (2000), Accuracy assessments of aerosol optical properties retrieved from AERONET Sun and sky-radiance measurements, *J. Geophys. Res.*, *105*, 9791–9806.

Dubovik, O., B. Holben, T. Eck, A. Smirnov, Y. Kaufman, M. King, D. Tanre, and I. Slutsker (2002), Variability of absorption and optical properties of key aerosol types observed in worldwide locations, *J. Atmos. Sci.*, *59*, 590–608.

Dunion, J., and C. Velden (2004), The impact of the Saharan air layer (SAL) on Atlantic tropical cyclone, *Bull. Am. Meteorol. Soc.*, *85*, 353–364.

European Centre for Medium-Range Weather Forecasts (2004), IFS documentation, technical report, Reading, U. K. (Available at http://www.ecmwf.int/research/ifsdocs/)

Food and Agricultural Organization (1988), UNESCO soil map of the world, *World Soil Resour. Rep.*, *60*, Rome.

Fouquart, Y., and B. Bonnel (1980), Computation of solar heating of the Earth's atmosphere: A new parameterization, *Contrib. Atmos. Phys.*, *53*(1), 35–62.

Geiger, B., C. Meurey, D. Lajas, L. Franchistéguy, D. Carrer, and J. L. Roujean (2008), Near real-time provision of downwelling shortwave radiation estimates derived from satllite observations, *Meteorol. Appl.*, in press.

Greed, G., J. Haywood, S. Milton, A. Keil, S. Christopher, P. Gupta, and E. Highwood (2008), Aerosol optical thicknesses over North Africa: 2. Modeling and model validation, *J. Geophys. Res.*, doi:10.1029/2007JD009457, in press.

Grini, A., P. Tulet, and L. Gomes (2006), Dusty weather forecasts using the MesoNH mesoscale atmospheric model, *J. Geophys. Res.*, *111*, D19205, doi:10.1029/2005JD007007.

Haywood, J., V. Ramaswamy, and B. Soden (1999), Tropospheric aerosol climate forcing in clear sky satellite observation over the oceans, *Science*, *283*, 1299–1303.

Holben, D., et al. (2001), An emerging ground-based aerosol climatology: Aerosol optical depth from AERONET, *J. Geophys. Res.*, *106*(D11), 12,067–12,097.

Houghton, J., Y. Ding, D. J. Griggs, M. Noguer, P. J. van der Linden, X. Dai, K. Maskell, and C. A. Johnson (Eds.) (2001), *Climate Change 2001*, pp. 392–393, Cambridge Univ. Press, Cambridge, U. K.

Joseph, J., W. Wiscombe, and J. A. Weinman (1976), The Delta-Eddington approximation for radiative flux transfer, *J. Atmos. Sci.*, *33*, 2452–2459.

Lafore, J., et al. (1998), The Meso-NH atmospheric simulation system. Part I: Adiabatic formulation and control simulations, *Ann. Geophys.*, *16*, 90–109.

Lohmann, U., and D. Diehl (2006), Sensitivity studies of the importance of dust ice nuclei for the indirect aerosol effect on stratiform mixed-phase clouds, *J. Atmos. Sci.*, *63*, 968–982.

Lothon, M., F. Said, F. Lohou, and B. Campistron (2008), Observation of the diurnal cycle in the low troposphere of West Africa, *Mon. Weather Rev.*, in press.

Marticorena, B., and G. Bergametti (1995), Modeling of the atmospheric dust cycle: 1. Design of a soil derived dust emission scheme, *J. Geophys. Res.*, *100*, 16,415–16,429.

Masson, V. (2000), A physically-based scheme for the urban energy balance in atmospheric models, *Boundary Layer Meteorol.*, *94*, 357–397.

Masson, V., J. Champeaux, F. Chauvin, C. Meriguet, and R. Lacaze (2003), A global database of land surface parameters at 1-km resolution in meteorological and climate models, *J. Clim.*, *16*(9), 1261–1282.

Milton, S., G. Greed, M. Brooks, J. Haywood, B. Johnson, R. Allan, and A. Slingo (2008), Modeled and observed atmospheric radiation balance during the West African dry season: Role of mineral dust, biomass burning aerosol, and surface albedo, *J. Geophys. Res.*, doi:10.1029/2007JD009741, in press.

Morcrette, J., and Y. Fouquart (1986), The overlapping of cloud layers in shortwave radiation parameterizations, *J. Atmos. Sci.*, *43*(4), 321–328.

Nickling, W., and J. Gillies (1989), Emission of fine-grained particulates from desert soils, in *Paleoclimatology and Paleometeorology: Modern and Past of Global Atmospheric Transport*, edited by M. Leinen and M. Sarnthein, pp. 133–165, Kluwer Acad., Dordrecht, Netherlands.

Noilhan, J., and J. Mahfouf (1996), The ISBA land surface parameterization scheme, *Global Planet. Change*, *13*, 145–159.

Parker, D., A. Diongue, R. Ellis, M. Felton, C. Taylor, C. Thorncroft, and P. Bessemoulin (2005), The diurnal cycle of the West African monsoon circulation, *Q. J. R. Meteorol. Soc.*, *131*, 2839–2860.

Redelsperger, J., D. Thorncroft, A. Diedhiou, T. Lebel, D. Parker, and J. Polcher (2006), African monsoon multiplidisciplinary analysis: An international research project and field campaign, *Bull. Am. Meteorol. Soc.*, *87*, 1739–1746.

Schepanski, K., I. Tegen, B. Laurent, B. Heinold, and A. Macke (2007), A new Saharan dust source activation frequency map derived from MSG-SEVIRI IR-channels, *Geophys. Res. Lett.*, *34*, L18803, doi:10.1029/2007GL030168.

Schmetz, J., P. Pili, S. Tjemkes, D. Just, J. Kerkmann, S. Rota, and A. Ratier (2002), An introduction to Meteosat second generation (MSG), *Bull. Am. Meteorol. Soc.*, *83*, 977–992.

Shao, Y., M. Raupach, and P. A. Findlater (1993), The effect of saltation bombardment on the entrainment of dust by wind, *J. Geophys. Res.*, *98*, 12,719–12,726.

Slingo, A., et al. (2006), Observations of the impact of a major Saharan dust storm on the atmospheric radiation balance, *Geophys. Res. Lett.*, *33*, L24817, doi:10.1029/2006GL027869.

Suhre, K., et al. (1998), Physico-chemical modeling of the First Aerosol Characterization Experiment (ACE 1) Lagrangian B: 1. A moving column approach, *J. Geophys. Res.*, *103*(D13), 16,433–16,455.

Tompkins, A. M., C. Cardinali, J.-J. Morcrette, and M. Rodwell (2005), Influence of aerosol climatology on forecasts of the African easterly jet, *Geophys. Res. Lett.*, *32*, L10801, doi:10.1029/2004GL022189.

Tulet, P., V. Crassier, F. Solmon, D. Guedalia, and R. Rosset (2003), Description of the Mesoscale Nonhydrostatic Chemistry model and application to a transboundary pollution episode between northern France and southern England, *J. Geophys. Res.*, *108*(D1), 4021, doi:10.1029/2000JD000301.

Tulet, P., V. Crassier, F. Cousin, K. Suhre, and R. Rosset (2005), ORILAM, a three-moment lognormal aerosol scheme for mesoscale atmospheric model: Online coupling into the Meso-NH-C model and validation on the Escompte campaign, *J. Geophys. Res.*, *110*, D18201, doi:10.1029/2004JD005716.

Zender, C. S., H. Bian, and D. Newman (2003), Mineral Dust Entrainment and Deposition (DEAD) model: Description and 1990s dust climatology, *J. Geophys. Res.*, *108*(D14), 4416, doi:10.1029/2002JD002775.

A. Boone and P. Tulet, Meteo-France, CNRM, GAME, 42 Gaspard Coriolis, F-31057 Toulouse, France. (aaron.boone@meteo.fr; pierre.tulet@meteo.fr)

M. Mallet and V. Pont, Laboratoire d'Aérologie, 14 Avenue Edouard Belin, F-31400 Toulouse, France. (marc.mallet@aero.obs-mip.fr; veronique.pont@aero.obs-mip.fr)

J. Pelon, Service d'Aéronomie, Universite Pierre et Marie Curie, Tour 45, 4 Place Jussieu, F-75252 Paris CEDEX 5, France. (jacques.pelon@aero.jussieu.fr)